

# POWER FLOW ANALYSIS AND CROSS-CURRENT OPTIMISATION FOR PARALLEL CONNECTED INVERTERS

TAHAR ZEBBADJI<sup>1</sup>, RACHID IBTIOUEN<sup>1</sup>, SEDDIK HADJI<sup>1</sup>

**Key words:** Grid-tied, Parallel inverters, Line impedance, Power flow, Uniform current distribution, Optimal circulating current.

The paper examines the impact of the line impedance of  $n$  parallel-connected inverters on the power flow, current distribution and circulating current among the units. Meanwhile, the previous research investigates either the case of inductive or resistive aspect for no more than three inverters connected in parallel. We figure out, for any number  $n$  of parallel inverters, the power flow with respect to the coupling impedance that meets the required inverter mode of operation: coupling impedance conditions are established. Furthermore, different line impedance from one inverter to the common point of connection contributes to a non-uniform output current distribution, which might exceed the ratings of the units. In addition, impedance difference from one phase to another of a given inverter induces a circulating current. To avoid such problems, new sinusoidal pulse width modulation (SPWM) strategy where parameters are found analytically is developed. First, a uniform current distribution independently of their number  $n$  and their line impedance is achieved. Second, an optimal circulating current with respect to the line impedance of each single unit is attained. Simulation is performed to validate analytical results.

## 1. INTRODUCTION

One of the world's biggest concerns is the need of sufficient energy that fits with the growth of the global population. With this increasing demand of power, more flexible, reliable, scalable and efficient systems are necessary [1]. Paralleling inverters happens to be the most suitable solution to convert renewable energy at a consumer level [2, 3]. This configuration gives the ability to convert much higher energy than single inverter [4].

For an effective paralleling, the inverters must share the total output power so that we can maintain as high as possible the system's performances. As the number of modules increases, it is possible to connect low power units. This leads to the use of common and mature components. Moreover, these converters can operate at relatively high frequencies with acceptable efficiency [5].

The proposed circuit (Fig. 1) consists of  $n$ -three phase inverters connected in parallel where the dc input voltage  $V_g$  is applied to the  $n$  units through an input inductance  $L_{in}$  [6]. The terminal of this inductance is then connected to the  $n$ -parallel inverters by means of an input capacitor  $C$  where  $i_{in}$  denotes the dc input current. The  $k^{th}$  three-phase inverter is in general connected to the common point of connection by a three-phase line impedance ( $R_{ak} + j\omega L_{ak}$ ,  $R_{bk} + j\omega L_{bk}$  and  $R_{ck} + j\omega L_{ck}$ ). The load consists of a three phase infinite bus (represented respectively by a balanced three phase sinusoidal voltage  $e_a$ ,  $e_b$  and  $e_c$ ) connected to the common point of connection in series with a three phase grid impedance ( $R_a + j\omega L_a$ ,  $R_b + j\omega L_b$  and  $R_c + j\omega L_c$ ) [7, 8]. Hence, the three-phase current flowing respectively in the  $k^{th}$  inverter and the grid are denoted by " $i_{ak}$ ,  $i_{bk}$ ,  $i_{ck}$ " and " $i_a$ ,  $i_b$ ,  $i_c$ ".

Stability analysis and performance evaluation of the overall circuit require modeling. In this study, the well-known average phase-leg technique is used [9]. The analysis of the average model has made possible the finding of the analytical solution. The objective of the analytical solution is to examine between system parameters and establish the power flow equation, as the line and grid impedance vary, from the  $n$  inverters and the grid.

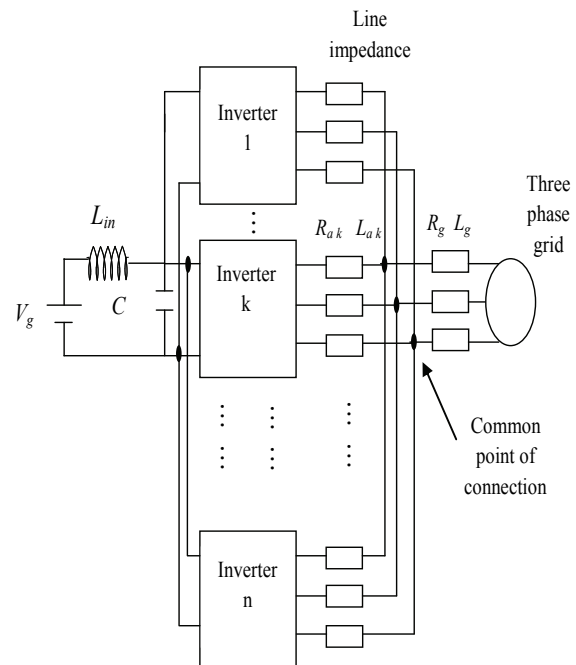


Fig. 1 – Circuit configuration for the grid tied parallel inverters with line and grid impedances

In [6], the analysis shows that the common point of connection of the  $n$  parallel inverters should be as close as possible to the grid. This will guarantee the main advantage of paralleling inverters. Furthermore, the variation of the coupling impedance may completely alter the mode of operation of the system.

In this paper, both the resistance and the reactance of the line and grid are taken into consideration to not compromise the inverter mode of operation. Then, the effects of the line impedance on the current distribution and the circulating current are analyzed.

In the last two decades, since renewable energy and micro-grid have gained a considerable interest, interconnection with different line parameters is subject to studies. The research concentrates on the effects of the grid and line impedance, on the active and reactive power, at

<sup>1</sup> Laboratoire de Recherche en Electrotechnique (LRE), Ecole Nationale Polytechnique (ENP), El-Harrach, Alger 16200. tahar.zebbadji@g.enp.edu.dz

both the inverter and grid terminals. In most studies, line and grid resistances are neglected, and only the line and grid reactance effects are taken into account. In the present work, to not alter the inverter operation mode, both line and grid resistance and reactance are taken into consideration. Then, the effects of the line impedance on the current distribution and the circulating current are analyzed.

The general circuit, used to analyze the parallel connection of  $n$  inverters to the grid, is presented in Section 2. In Section 3, the power flow between the dc and ac grid with respect to either the line or the grid impedance is analyzed for any number of inverters. In Section 4, the load current distribution along the inverters is investigated. Finally, in Section 5, the circulating current is analyzed for the case where the line impedance of a given phase is different from that of the other phases.

## 2. ANALYSIS OF THE N PARALLEL CONNECTED INVERTERS TO THE GRID

In [6, 7], we have shown the impact of the line and grid impedance, the number  $n$  of parallel inverters etc. on the operating mode and performance of the circuit. The main advantage of paralleling inverters is guaranteed if the ratio of grid impedance to line impedance is small. Furthermore, an appropriate selection of various parameters ensures that the system's inverter operation mode is not compromised. Analysis of different transfer functions highlighted the impact of circuit parameters on system performances. Increasing the number of inverters allows the reduction of the overshoot and the time input voltage response. Taking into account the grid impedance ( $Z_g \neq 0$ ), the input current increase is no longer proportional to the number of inverters connected in parallel.

If all the phases have equal impedance value, those of the  $k^{\text{th}}$  inverter and the grid are as follows:

$$\left. \begin{aligned} R_{ai} &= R_{bi} = R_{ci} = R_{lk} \\ R_a &= R_b = R_c = R_g \\ L_{ai} &= L_{bi} = L_{ci} = L_{lk} \\ L_a &= L_b = L_c = L_g \end{aligned} \right\} \quad (1)$$

Using the phase-leg technique to the circuit described previously, one can obtain the following equations:

$$\left. \begin{aligned} L_{in} \frac{di_{in}}{dt} &= V_g - V \\ C \frac{dV}{dt} &= i_{in} - \sum_{k=1}^n d_{3k-2} i_{ak} - \sum_{k=1}^n d_{3k-1} i_{bk} - \sum_{k=1}^n d_{3k} i_{ck} \\ L_{ai} \frac{di_{ai}}{dt} &= d_{3k-2} V - L_g \sum_{k=1}^n \frac{di_{ak}}{dt} - R_g \sum_{k=1}^n i_{ak} - R_{ai} i_{ai} - e_a + V_{N'N} \\ L_{bi} \frac{di_{bi}}{dt} &= d_{3k-1} V - L_g \sum_{k=1}^n \frac{di_{bk}}{dt} - R_g \sum_{k=1}^n i_{bk} - R_{bi} i_{bi} - e_b + V_{N'N} \\ L_{ci} \frac{di_{ci}}{dt} &= d_{3k} V - L_g \sum_{k=1}^n \frac{di_{ck}}{dt} - R_g \sum_{k=1}^n i_{ck} - R_{ci} i_{ci} - e_c + V_{N'N} \end{aligned} \right\} \quad (2)$$

where  $V$  is the voltage across the input capacitance and  $V_{N'N}$  is the common mode voltage.  $d_{3k-2}$ ,  $d_{3k-1}$  and  $d_{3k}$  are the

phase-leg duty cycles of a sinusoidal pulse width modulation (SPWM) for the  $k^{\text{th}}$  inverter in synchronism with the grid [8] such that:

$$\left. \begin{aligned} d_{3k-2} &= \frac{1}{2} \left[ 1 + d_{mk} \cos(\omega t - \varphi_k) \right] \\ d_{3k-1} &= \frac{1}{2} \left[ 1 + d_{mk} \cos(\omega t - \varphi_k - \frac{2\pi}{3}) \right] \\ d_{3k} &= \frac{1}{2} \left[ 1 + d_{mk} \cos(\omega t - \varphi_k + \frac{2\pi}{3}) \right] \end{aligned} \right\} \quad (3)$$

where  $d_{mk}$  and  $\varphi_k$  are, respectively, the modulation index and the phase shift of duty cycles as referred to the grid.

Applying the Park transform to the above system of equations, we obtain the following expressions:

$$\left. \begin{aligned} C \frac{dV}{dt} &= i_{in} - \sum_{k=1}^n d_{dk} i_{dk} - \sum_{k=1}^n d_{qk} i_{qk} - \sum_{k=1}^n d_{zk} i_{zk} \\ L_{lk} \frac{di_{dk}}{dt} &= d_{dk} V + L_{lk} \omega i_{qk} + L_g \omega \sum_{k=1}^n i_{qk} - L_g \sum_{k=1}^n \frac{di_{dk}}{dt} \\ &\quad - R_g \sum_{k=1}^n i_{dk} - R_{lk} i_{dk} - e_{dl} \\ L_{lk} \frac{di_{qk}}{dt} &= d_{qk} V - L_{lk} \omega i_{dk} - L_g \omega \sum_{k=1}^n i_{dk} - L_g \sum_{k=1}^n \frac{di_{qk}}{dt} \\ &\quad - R_g \sum_{k=1}^n i_{qk} - R_{lk} i_{qi} - e_{ql} \\ L_{lk} \frac{di_{zk}}{dt} &= d_{zk} V - L_{lk} \omega i_{dk} - R_{lk} i_{zqi} - e_{zl} - \sqrt{3} V_{N'N}' \end{aligned} \right\} \quad (4)$$

where  $e_{dl}$ ,  $e_{ql}$  and  $e_{zl}$  are respectively the direct, indirect and zero sequence components of the line to line grid voltages;  $i_{dk}$ ,  $i_{qk}$  and  $i_{zk}$  are those of the line to line currents of the  $k^{\text{th}}$  inverter while  $d_{dk}$ ,  $d_{qk}$  and  $d_{zk}$  are those of the phase leg duty cycles.

From equations (4), one can derive the average circuit model of the  $n$  parallel-connected inverters to the grid in the  $dq$  coordinate. With some assumptions, a simplified model is obtained by either reflecting all the variables to the dc or ac side. For instance, if we are interested in the dc input current to check whether uniform current distribution is attained along the  $n$  inverters, we should solve the circuit reflected to the dc side. This study cannot tell if the desired operation mode is reached or not: power flow analysis has to be conducted.

## 3. POWER FLOW ANALYSIS OF THE N PARALLEL CONNECTED INVERTERS

One of the main issues of grid tied inverter is the control of the injected active and reactive power to the three-phase grid [10–13]. For the parallel case, both the lines and grid impedances play an important role in the average active and reactive power transfer. In this section, we determine the analytical expressions for the average power with respect to the circuit parameters and give a particular emphasis to the nature of impedance. The analysis of the system is conducted by assuming that all the inverters are controlled by similar SPWM and all the line impedances are identical,

such that:

$$\left. \begin{aligned} R_{ai} &= R_{bi} = R_{ci} = R_l \\ R_a &= R_b = R_c = R_g \\ L_{ai} &= L_{bi} = L_{ci} = L_l \\ L_a &= L_b = L_c = L_g \end{aligned} \right\}. \quad (5)$$

The expression of the average active and reactive power is obtained by first solving the analytical expressions of the state variable of the circuit represented in Figure 1. This will lead to the following expressions in the frequency domain:

$$\left. \begin{aligned} i_d(s) &= \frac{\frac{d_m}{2} ((R_T + sL_T) \cos \varphi - L_T \omega \sin \varphi) V_g(s) - \frac{(R_T + sL_T) e_d(s)}{(R_T + sL_T)^2 + L_T^2 \omega^2}}{(R_T + sL_T)^2 + L_T^2 \omega^2} \\ i_q(s) &= \frac{\frac{d_m}{2} ((R_T + sL_T) \sin \varphi + L_T \omega \cos \varphi) V_g(s) - \frac{L_T \omega e_d(s)}{(R_T + sL_T)^2 + L_T^2 \omega^2}}{(R_T + sL_T)^2 + L_T^2 \omega^2} \end{aligned} \right\}, \quad (6)$$

where

$$\left. \begin{aligned} X_T &= (L_g + \frac{L_L}{n}) \omega \\ R_T &= R_g + \frac{R_L}{n} \end{aligned} \right\}. \quad (7)$$

-  $X_T$ ,  $X_g$  and  $X_L$  are respectively the coupling, grid and line reactances.

-  $R_T$ ,  $R_g$  and  $R_L$  are respectively the coupling, grid and line resistances.

-  $d_m$  and  $\varphi$  are respectively the modulation index of duty cycle and its phase shift with respect to grid voltage.

From equations (6), one obtains the steady state output phase current as follows:

$$I_a = \frac{1}{\|Z_T\|} \left( \frac{d_m}{2} V_g \cos \left( \omega t - \frac{\pi}{6} - \varphi - \theta \right) - V_m \cos \left( \omega t - \frac{\pi}{6} - \theta \right) \right), \quad (8)$$

where  $Z_T$  and  $\theta$  are the coupling impedance and its argument.  $V_m$  is the maximum line to neutral grid voltage.

Equation (8) describes similar behavior to that of the synchronous machine, having a terminal voltage equal to  $(d_m V_g)/2$  feeding an infinite bus  $V_m$  through a coupling impedance  $Z_T$ , which is in fact a combination of the grid and a fraction of the line impedances. The infinite bus is taken as a reference.

Special care is required to ensure that changes in circuit parameter's settings do not undermine the operation mode of the structure. This condition places a restriction on a possible variation of the structure components such that the overall circuit would not shift from the authorized operation mode. This makes the power flow a major concern of the

following analysis.

The average reactive and active power can flow in either direction depending on circuit parameters. The active power should flow in a way such that it does not compromise the inverter mode of the overall circuit. Basic equations in power flow system, which relate the active and the reactive power delivered respectively by the parallel inverter ( $P_1$  and  $Q_1$ ) and the grid terminals ( $P_2$  and  $Q_2$ ) are as follow:

$$\left. \begin{aligned} P_1 &= \frac{R_T A - 2R_T B \cos \varphi - 2X_T B \sin \varphi}{4 Z_T^2} \\ P_2 &= \frac{-2R_T V_m^2 + R_T B \cos \varphi - X_T B \sin \varphi}{2 Z_T^2} \\ Q_1 &= \frac{X_T A - 2X_T B \cos \varphi + 2B R_T \sin \varphi}{4 Z_T^2} \\ Q_2 &= \frac{-2X_T V_m^2 + R_T B \sin \varphi + X_T B \cos \varphi}{2 Z_T^2} \end{aligned} \right\}, \quad (9)$$

where

$$\left. \begin{aligned} A &= d_m^2 V_g^2 \\ B &= d_m V_g V_m \end{aligned} \right\}. \quad (10)$$

The analysis shows the variation of the average active and reactive power with respect to either the coupling resistance or inductance. In this particular case, one notices that even though, for some line and grid resistance, the  $n$ -parallel inverters operate in the inverter mode, the system is not able to deliver active power to the grid. For this reason, we cannot tell if the overall structure is or is not delivering active power to the grid just by analyzing the dc input current. One should examine how the power is flowing in both terminals of the circuit. To overcome this situation and let the parallel inverters convert energy from the dc side to the utility, one has to adjust the SPWM parameters and choose an appropriate dc input voltage.

In the case of a photovoltaic structure, a proper output voltage of the dc converter (which is in fact the input voltage to the  $n$  parallel inverters) can overcome this particular situation. As depicted in Figs. 2, 3, 4 and 5, the structure parameters (given in Table 1) can supply a positive or a negative active power to the grid.

Table 1  
Circuit parameters

Input voltage	$V_g = 700$ V
Input filter	$L_{in} = 80$ mH, $C = 6$ mF
Inverter parameters	$\varphi = -0.1$ rad, $d_m = 0.8$ , $n = 3$
Line parameters	$L_l = 0.6$ mH, $R_l = 20$ m $\Omega$
Three phase grid	$V_m = 220\sqrt{2}$ V, $R_g = 10$ m $\Omega$ , $L_g = 0.3$ mH

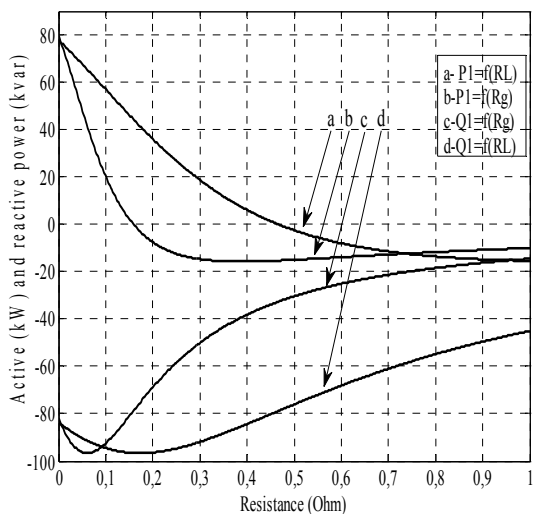


Fig. 2 – Variation of the active and reactive power supplied by three parallel inverters with respect to the line and grid resistance.

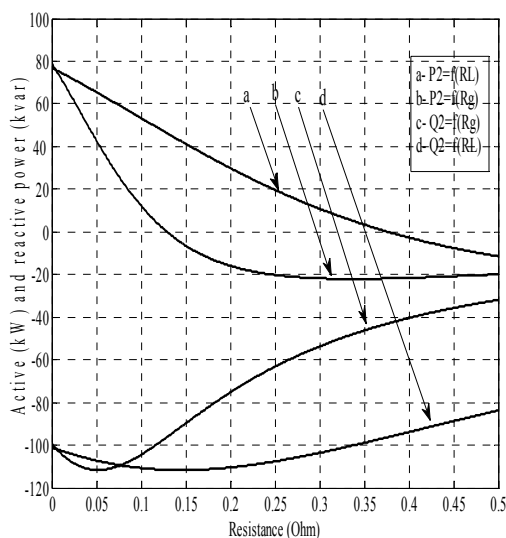


Fig. 4 – Variation of the active and reactive power at the grid terminal with respect to the line and grid resistance.

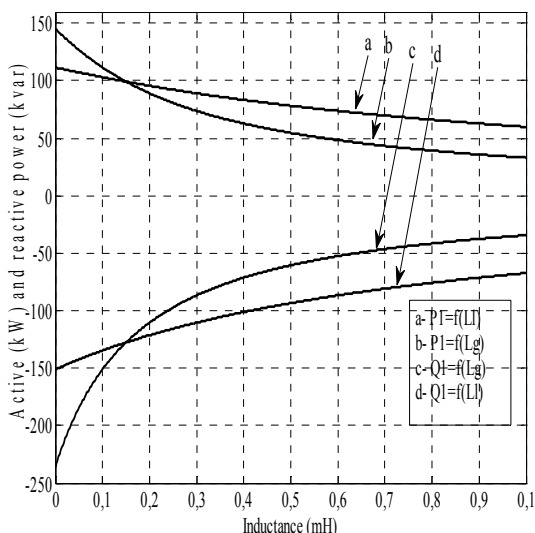


Fig. 3 – Variation of the active and reactive power supplied by three parallel inverters with respect to the line and grid inductance.

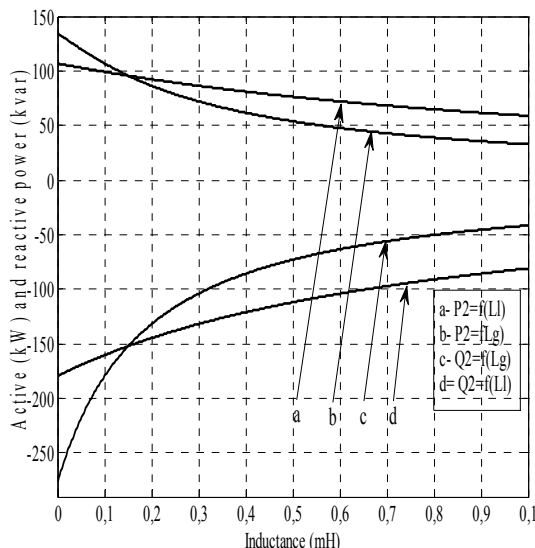


Fig. 5 – Variation of the active and reactive power at the grid terminal with respect to the line and grid inductance.

From these graphs, we figure out the maximum values, of either the line or the grid impedances, to comply with the intended operation mode of the structure. For a grid resistance equal to 10 mΩ, a positive active power flow to the grid (Fig. 4) requires a line resistance smaller than 0.376 Ω. Whereas, for a line resistance of 20 mΩ, positive active power flow to the grid imposes a grid resistance less than and 0.129 Ω.

For an acceptable efficiency (*i.e.* greater than 97 %), a coupling resistance smaller than 16.6 mΩ is required: this corresponds to a grid resistance of 10 mΩ and a line resistance of 20 mΩ for three-parallel inverters.

#### 4. UNBALANCE IN LINE IMPEDANCE EFFECT ON THE OUTPUT CURRENT DISTRIBUTION

In the previous analysis, we have considered the case where all the identical inverters are connected to the common connection point by equal line impedance. This configuration ensures uniform distribution of the active and reactive power along the  $n$  parallel inverters [14] and exhibits a non-zero circulating current [15].

- What happens if one of the line-phase impedance of a given inverter is different from those of the line-phases?
- What is the effect of a different line impedance of a given inverter on the load current distribution among the  $n$  inverters?

If all the coupling impedances are equal and an identical SPWM is applied to all the units, then each phase will carry the same current. If not, the phase with different coupling impedance has to be powered by a different phase voltage such that this will make its phase current take a value equal to that of the other phases. In the open loop case, such an adjustment should be done by an appropriate choice of the modulation index and phase to minimize the circulating current. A simulation performed under Matlab/Simulink environment is conducted to prove whether the adjusted SPWM analytical parameters are in good agreement or not with these results.

Figure 6 shows the current distribution for the case of three inverters connected in parallel in which the line impedances of the first inverter are three times those of the second inverter. The first, second and the third unit must withstand respectively 18 %, 55 % and 27 % of the load current (which is equal to 275 A). The current of the second inverter exceeds the desired 33 % of the load current ratings by more than 166 %. This particular situation compromises the uniform current-distribution principle. Furthermore, this might lead to a decrease in the overall efficiency. A sinusoidal PWM technique is developed to select the modulation parameters, which enable a fair distribution of the load current between the  $n$  parallel-connected inverters and do not compromise the system mode of operation. For a change in the coupling impedance from  $Z_T$  to  $Z_T'$ , what should be the new SPWM parameters which ensure an identical phase line current in every inverter? From equation (8) and keeping an equal phase current, we obtain the appropriate phase and modulation index of the SPWM as follows:

$$\left. \begin{aligned} d_m' &= 2 \sqrt{\frac{V_m^2 + \frac{Z_T'^2 \alpha}{Z_T^2} - 2V_m \frac{Z_T'}{Z_T} \sqrt{\alpha} \cos \xi}{V_g}} \\ \phi' &= \cos^{-1} \left( \frac{V_m^2 + \frac{d_m'^2 V_g^2}{4} - \frac{Z_T'^2 \alpha}{Z_T^2}}{V_m d_m' V_g} \right) \end{aligned} \right\} \quad (11)$$

With a different line impedance, the application of this strategy leads to a uniform current distribution between the  $n$  parallel-connected inverters. Figure 7 illustrates the case where the line impedances of the first and the third inverter are respectively equal to three and two times the line impedances of the second one. For the steady state response, an appropriate choice of the SPWM parameters ( $d_m' = 0.7358$  instead of 0.8 and  $\phi' = -0.1966$  rad instead of  $-0.1$  rad for the first inverter and  $d_m' = 0.767$  instead of 0.8 and  $\phi' = -0.1463$  rad instead of  $-0.1$  rad for the third one) guarantees an equal sharing of the load current between the three units.

## 5. CIRCULATING CURRENT MINIMIZATION UNDER UNBALANCE IN LINE IMPEDANCE

The case of  $n$ -identical inverters connected in parallel to a grid with equal line impedances, led to a non-circulating

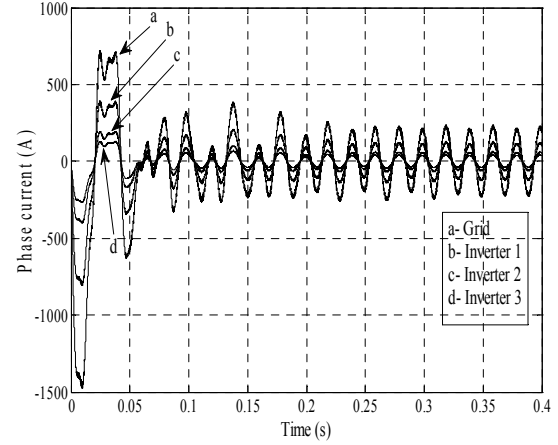


Fig. 6 – Current distribution for three parallel-connected inverters with line impedance  $Z_{L1} = 3Z_{L2}$  and  $Z_{L3} = 2Z_{L2}$  and identical SPWM parameters

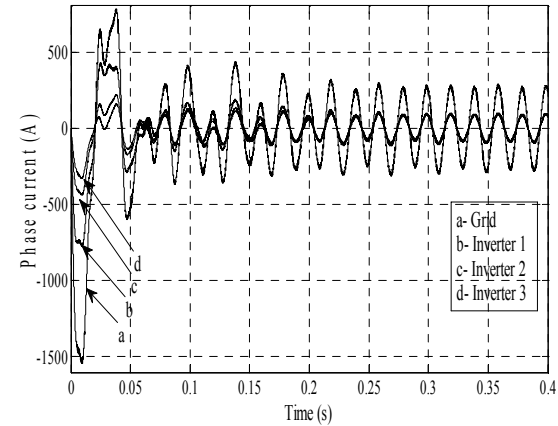


Fig. 7 – Current distribution for three parallel-connected inverters with a line impedance  $Z_{L1} = 3Z_{L2}$  and  $Z_{L3} = 2Z_{L2}$  and adjusted SPWM parameters

current between the  $n$  inverters. This is because the inverters produce an equal line to neutral voltage that powers the same line to neutral grid voltage. Then, we obtain an equal current sharing of current flowing into the grid along the  $n$  inverters.

The circulating current  $I_{cr,1}$  [16–18] flowing in the first inverter for  $n$  parallel-connected inverters is defined as:

$$I_{cr,1} = \frac{\sum_{i=1}^n I_{a i} + \sum_{i=1}^n I_{b i} + \sum_{i=1}^n I_{c i}}{n} \quad (12)$$

Equation (12) shows clearly that for an ideal structure, all the phase currents are equal in amplitude and, hence, the circulating current is null. So if all the phases having the same coupling impedance  $Z_T$  are controlled by an equal set of  $d_m$  and  $\phi$ , and the ones having  $Z_T'$  controlled by the new SPWM parameters  $d_m'$  and  $\phi'$ , the circulating current reaches its optimal status.

A system of three-parallel inverters with the second one having a different phase line impedance (*i.e.* phase “a”) gives a steady state circulating current amplitude equal to 33 A (Fig. 8 a). From Equation (11) we calculate the new modulation parameters ( $\phi' = -0.1966$  rad and  $d_m' = 0.7358$ ) to be applied to the phase-leg which presents a different line impedance. Figure 8 shows maximum amplitude of 3 A (Fig. 8 b): the circulating current is reduced by a factor of 90 %.

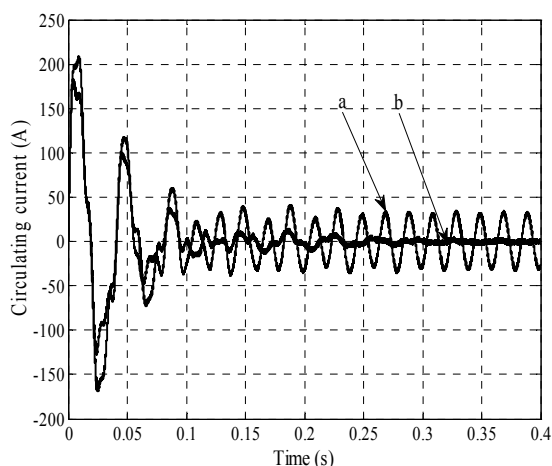


Fig. 8 – Circulating current for three parallel-connected inverters with  $Z_{L_a} = 3Z_{L_b} = 3Z_{L_c}$ : a)  $\varphi = -0.1$  rad and  $d_m = 0.8$ , b)  $\varphi' = -0.1966$  rad and  $d_m' = 0.7358$ .

## 6. CONCLUSIONS

The power flow between the common connection point and the grid shows the active or reactive power flow to the ac grid. The application of the average-leg technique makes possible the use of an average model to obtain the analytical solution of the parallel inverter for any number of inverters. We can establish the required limits of this coupling impedance to ensure a proper mode of operation of the  $n$  parallel-connected inverters. This will not compromise the main objective of the overall circuit, which is the power transfer from the dc to ac bus.

We highlighted the importance of the line impedance effect of every single inverter on the load current distribution. Different line impedance connected to the common connection point causes non-uniform load current distribution. This can lead to a situation where it would exceed the rating limits of this inverter. Therefore, we have established analytical SPWM parameters with respect to the coupling impedance to restore the load current sharing principle. This will guarantee that all the inverters operate under equal power load that does not exceed their intended rated power.

Different phase line impedances of an inverter induce circulating current. The established analytical solutions with judicious choice of the SPWM parameters enable minimizing the circulating currents. This will contribute to eliminate the low frequency component of the circulating currents. A considerable reduction of the circulating current and an increase in the overall circuit efficiency are obtained. Simulation is performed to validate analytical results.

Received on May 19, 2017

## REFERENCES

1. I. Felea, V. Moldovan, D. Albut, *Specificities in analysis of energy availability generated by photovoltaic sources*, Rev. Roum. Sci. Techn. – Électrotechn. et Énerg., **61**, 1, pp. 42–47 (2016).
2. L. Zhang, K. Sun, Y. Xing, J. Zhao, *Parallel operation of modular single-phase transformerless grid-tied PV inverters with common DC bus and AC bus*, IEEE Journal of Emerging and Selected Topics in Power Electronics, **99**, pp. 1–7 (2015).
3. O. Ellabban, H. Abu-Rub, F. Blaabjerg, *Renewable energy resources: Current status, future prospects and their enabling technology*, Renew Sust. Energ. Rev., **39**, pp. 748–764 (2014).
4. H.K. Krishnamurthy, R. Ayyanar, *Building block converter module for universal (AC-DC, DC-AC, DC-DC) fully modular power conversion architecture*, IEEE 2007 Power Electronics Specialists Conference, Orlando, USA, (2007).
5. J.W. Kolar, Krismer F, Lobsiger Y, Muhlethaler J, Nussbaumer T, Minibok J. *Extreme efficiency power electronics*, 7th International Conference on Integrated Power Electronics Systems, Nuremberg, Germany, (2012).
6. T. Zebbadji, S. Hadji, R. Ibtouen. *Line and grid impedance impact on the performances of parallel modular inverter system*, International Journal of Power Electronics and Drive systems, **6**, pp. 100–108 (2015).
7. T. Zebbadji, S. Hadji, R. Ibtouen, *A simple average model and analysis of an n parallel-connected inverters*, 15<sup>th</sup> IEEE Workshop on Control and Modeling of Power Electronics, Santander, Spain, pp. 1–8 (2014).
8. T. Zebbadji, R. Ibtouen, S. Hadji, *Optimum SPWM parameters for unbalanced grid voltage of n parallel-connected inverters*, 19<sup>th</sup> IEEE International Power Electronics and Motion Control, Varna, Bulgaria, pp. 180–185 (2016).
9. R. Li, D. Xu, *Parallel operation of full power converters in permanent-magnet direct-drive wind power generation system*, IEEE Trans. Ind. Electron., **60**, pp. 1619–1629 (2013).
10. I. V. Nemoianu, R. M. Ciuceanu, *Aspect of active and reactive powers conservation in three-phase circuits with zero impedance neutral and two nonlinear unbalanced loads*, Rev. Roum. Sci. Techn. – Électrotechn. et Énerg., **61**, 4, pp. 349–354, (2016).
11. M.N. Amrani, A. Dib, *Direct power control for a photovoltaic conversion chain connected to a grid*, Rev. Roum. Sci. Techn. – Électrotechn. et Énerg., **61**, 4, pp. 378–382, (2016).
12. N. Mohsenifar, A. Kargar, N. R. Abjadi, *Improved cascade sliding mode for power control in a microgrid*, Rev. Roum. Sci. Techn. – Électrotechn. et Énerg., **61**, 4, pp. 430–435, (2016).
13. Y. Chen, J. M. Guerrero, Z. Shuai, Z. Chen; L. Zhou; A. Luo, *Fast reactive power sharing, circulating current and resonance suppression for parallel inverters using resistive-capacitive Output impedance*, IEEE Transactions on Power Electronics, **31**, 8, pp. 5524–5537, (2016).
14. A. M. Roslan, K. H. Ahmed, S. J. Finney; B. W. Williams, *Improved instantaneous average current-sharing control scheme for parallel-connected inverter considering line impedance impact in microgrid networks*, IEEE Transactions on Power Electronics, **26**, 3, pp. 702–716, (2011).
15. K. Duwadi, N. Gyawali, R. Karki, *Design, modelling and simulation of improved power sharing scheme for parallel operation of VSI*, 12<sup>th</sup> IEEE International Conference on Control and Automation (ICCA), Kathmandu, Nepal, pp. 359–364 (2016).
16. X. Yan, Y. Zhang, W. Zhang, J. Tang, *Circulating-current analysis and power sharing control of parallel inverters with different capacities*, International Conference on Renewable Power Generation, Beijing, China, pp. 1–6 (2015).
17. T.P. Chen, *Zero-sequence circulating current reduction method for parallel HEPWM inverters between AC bus and DC bus*, IEEE Trans. Ind. Electron., **59**, pp. 290–300 (2012).
18. M. Zhang, Z. Du, X. Lin; J. Chen, *Control Strategy Design and Parameter Selection for Suppressing Circulating Current Among SSTs in Parallel*, IEEE Transactions on Smart Grid, **6**, 4, pp. 1602–1609 (2015).